Time-Synchronized Convolutional Perfectly Matched Layer for Improved Absorbing Performance in FDTD

Iraklis Giannakis and Antonios Giannopoulos

***Abstract*—A performance-enhancing modification to the convolutional perfectly matched layer (CPML) technique for implementing the complex frequency-shifted perfectly matched layer (CFS-PML) absorbing boundary condition is presented. By adopting this modification, an apparent discrepancy in the time synchronization between the CPML and the main finite-difference time-domain (FDTD) algorithm is resolved. This is achieved by employing a semi-implicit approach that synchronizes CPML with the main FDTD algorithm. It is shown through 2-D and 3-D numerical examples that the suggested modification to the CPML algorithm increases its performance without increasing its computational cost.**

***Index Terms*—Complex frequency-shifted PML (CFS-PML), convolutional PML (CPML), finite-difference time domain (FDTD), perfectly matched layer (PML), recursive integration PML (RIPML), stretched coordinate PML (SC-PML).**

I. Introduction

PERECTLY matched layer (PML), first introduced in 1994 by [1] and [2], has since become the most used and well-known absorbing boundary condition employed in finite-difference time-domain (FDTD) [3] electromagnetic modeling codes as well as in other numerical techniques like the finite-element time-domain method [4]. Different approaches for implementing PML in FDTD grids have been suggested, which can be roughly categorized into: split field formulations [1], stretched coordinate PMLs (SC-PMLs) [2], and uniaxial perfectly matched layer (UPML) [5]. The SC-PML is considered possibly as the most attractive choice for implementing PML for a lot of reasons. Among them, the most important are that it makes the understanding of PML easier [6]; it is easier to incorporate it in cylindrical and spherical coordinate systems [7]; and through SC-PML, more elegant implementations can be obtained, with which the PML is incorporated as a correction term [8], [9]. In addition, lossy, dispersive [10], and anisotropic [11] media can be easily treated. Finally, SC-PML makes the implementation of complex frequency-shifted PML (CFS-PML) more computationally efficient [12].

The CFS-PML was first introduced by [13] and has been proven [14] that it can be used in order to reduce the late time reflections that occur when using SC-PML [15]. It has been also shown that CFS-PML decreases the numerical reflections related to the overabsorption of the propagating evanescent waves inside the PML region [16], [17], [18].

In [12], an elegant and computationally efficient way to implement CFS-PML has been introduced. This method is based on an SC-PML formulation and is referred to as the convolutional perfectly matched layer (CPML). CPML uses a recursive convolution approach first introduced by [19] (aimed for implementing dispersive media in FDTD) to evaluate the convolution between the complex frequency-shifted stretching function and the spatial derivatives of the magnetic and the electric fields. An alternative interpretation of CPML based on an auxiliary differential equation (ADE) formulation is presented in [20]; both of them result in the same equations.

Different methods for evaluating a convolution recursively have been suggested since the first recursive convolution (RC) [19] method was proposed. Piecewise linear recursive convolution (PLRC) [21] and trapezoidal recursive convolution (TRC) [22] are considered second-order accurate algorithms [22] and have been proven more accurate than RC for both dispersive media [21] and PML [8] implementations. In contrast to standard RC, as introduced for modeling dispersive media, in CPML, a TRC approach is employed by default. This is a result of convolving spatial derivatives that are at half a time-step apart from the corresponding fields that are being updated by the FDTD equations. Therefore, CPML rivals other second-order accurate techniques based on recursive integration [8], bilinear transform [23], and Z-transform [24].

It has been shown, however, that in some examples CPML does not perform as well as other second-order PML methods [8]. A closer inspection of the algorithm reveals that this is not due to the order of accuracy of the numerically evaluated convolution, but due to the fact that the implemented CFS-PML by the CPML is not properly synchronized with the main FDTD algorithm. In this letter, a simple semi-implicit scheme is proposed that results in the synchronization of CPML with the main FDTD without increasing the computational cost. The improvement of the proposed synchronization on the overall performance of CPML is shown through 2-D and -3D numerical examples.

II. Semi-Implicit CPML

Maxwell's equations (in frequency domain) using CFS-PML can be written in general form as

$$j\omega\vec{D}_\omega = \nabla_s \times \vec{H}_\omega \tag{1}$$

$$j\omega\vec{B}_\omega = -\nabla_s \times \vec{E}_\omega \tag{2}$$

Manuscript received October 07, 2014; revised November 20, 2014; accepted November 25, 2014. Date of publication December 04, 2014; date of current version March 02, 2015. This work was supported by the U.K. Engineering and Physical Sciences Research Council (EPSRC) and the Defence Science and Technology Laboratory (DSTL).

The authors are with the School of Engineering, The University of Edinburgh, Edinburgh EH9 3JL, U.K. (e-mail: I.Giannakis@ed.ac.uk; A.Giannopoulos@ed.ac.uk).

Digital Object Identifier 10.1109/LAWP.2014.2376981

$$\nabla_s = \frac{1}{s_x}\frac{\partial}{\partial x}\vec{x} + \frac{1}{s_y}\frac{\partial}{\partial y}\vec{y} + \frac{1}{s_z}\frac{\partial}{\partial z}\vec{z} \tag{3}$$

$$s_u = \kappa_u + \frac{\sigma_u}{\alpha_u + j\omega\epsilon_0} \tag{4}$$

where $\vec{E}$ is the electric field; $\vec{H}$ is the magnetic field strength; $\vec{B}$ is the magnetic flux density; $\vec{D}$ is the electric flux density; ω is the angular frequency; j is the imaginary unit ($j = \sqrt{-1}$); $\nabla_s\times$ is the SC-PML curl operator; and κ_u, σ_u, and α_u are constants ($u \in \{x, y, z\}$) that define the complex frequency-shifted stretching function proposed in [13].

Transforming (1) and (2) to time domain results in

$$\frac{\partial \vec{D}}{\partial t} = \nabla_\kappa \times \vec{H} + \nabla_\zeta \times \vec{H} \tag{5}$$

$$\frac{\partial \vec{B}}{\partial t} = -\nabla_\kappa \times \vec{E} - \nabla_\zeta \times \vec{E} \tag{6}$$

$$\nabla_\kappa = \frac{1}{\kappa_x}\frac{\partial}{\partial x}\vec{x} + \frac{1}{\kappa_y}\frac{\partial}{\partial y}\vec{y} + \frac{1}{\kappa_z}\frac{\partial}{\partial z}\vec{z} \tag{7}$$

$$\nabla_\zeta = \zeta_x * \frac{\partial}{\partial x}\vec{x} + \zeta_y * \frac{\partial}{\partial y}\vec{y} + \zeta_z * \frac{\partial}{\partial z}\vec{z} \tag{8}$$

$$\zeta_u = -\frac{\sigma_u}{\epsilon_0\kappa_u^2} e^{-\left(\frac{\sigma_u}{\epsilon_0\kappa_u} + \frac{\alpha_u}{\epsilon_0}\right)t} \tag{9}$$

where $*$ denotes temporal convolution.

For the case of D_x, following the procedure described in [12] yields

$$\begin{aligned}\delta_{\Delta t}\left(D^{n+1/2}_{x_{i+\frac{1}{2},j,k}}\right) = {} & \frac{1}{k_y}\Lambda_{\Delta y}\left(H^{n+1/2}_{z_{i+\frac{1}{2},j,k}}\right) - \frac{1}{k_z}\Lambda_{\Delta z}\left(H^{n+1/2}_{y_{i+\frac{1}{2},j,k}}\right) \\ & + \sum_{m=0}^{n}\left(Z^m_{0,y}\Lambda_{\Delta y}\left(H^{n-m+1/2}_{z_{i+\frac{1}{2},j,k}}\right)\right. \\ & \left. - Z^m_{0,z}\Lambda_{\Delta z}\left(H^{n-m+1/2}_{y_{i+\frac{1}{2},j,k}}\right)\right)\end{aligned} \tag{10}$$

where $\delta_{\Delta t}$ is a second-order central difference operator in time [(11)], $\Lambda_{\Delta u}$ is a spatial second-order central difference operator [(12) and (13)], and $Z^m_{0,u}$ is the discrete impulse response of ζ_u [(14)] [12] as follows:

$$\delta_{\Delta t}\left(F^t_{u_{i,j,k}}\right) = \frac{F^{t+\frac{\Delta t}{2}}_{u_{i,j,k}} - F^{t-\frac{\Delta t}{2}}_{u_{i,j,k}}}{\Delta t} \tag{11}$$

$$\Lambda_{\Delta z}\left(F^t_{u_{i,j,k}}\right) = \frac{F^t_{u_{i,j,k+\frac{1}{2}}} - F^t_{u_{i,j,k-\frac{1}{2}}}}{\Delta z} \tag{12}$$

$$\Lambda_{\Delta y}\left(F^t_{u_{i,j,k}}\right) = \frac{F^t_{u_{i,j+\frac{1}{2},k}} - F^t_{u_{i,j-\frac{1}{2},k}}}{\Delta y} \tag{13}$$

$$\begin{aligned} Z^m_{0,u} &= \int_{m\Delta t}^{(m+1)\Delta t} \zeta_u(\tau)d\tau \\ &= -\frac{\sigma_u}{\epsilon_0\kappa_u^2}\int_{m\Delta t}^{(m+1)\Delta t} e^{-\left(\frac{\sigma_u}{\epsilon_0\kappa_u} + \frac{\alpha_u}{\epsilon_0}\right)\tau}d\tau \end{aligned} \tag{14}$$

$$= p_u e^{-\left(\frac{\sigma_u}{\kappa_u} + \alpha_u\right)\frac{m\Delta t}{\epsilon_0}}$$

$$p_u = \frac{\sigma_u}{\sigma_u\kappa_u + \kappa_u^2\alpha_u}\left(e^{-\left(\frac{\sigma_u}{\kappa_u} + \alpha_u\right)\frac{\Delta t}{\epsilon_0}} - 1\right). \tag{15}$$

The summation in (10) is calculated recursively by taking advantage of the exponential nature of Z_0 [19]. From (10) and (14), it is evident that the convolution in each time-step takes place from 0 to $(n+1)\Delta t$. The spatial derivatives are assumed to be constant at the intervals $[n\Delta t, (n+1)\Delta t]$, and they are equal with the value they have at $(n+1/2)\Delta t$. This approach for evaluating recursively the convolution is known as TRC [22], which is more accurate compared to the first-order RC suggested in [19] and rivals the accuracy [22] of PLRC [21]. The drawback of CPML is not the order of accuracy of TRC, but the fact that the approximated convolution is not synchronized with the main FDTD algorithm. This is evident in (10), in which the time derivative of the electric flux as well as the spatial derivatives of the magnetic field are evaluated at $(n+1/2)\Delta t$ (using a second-order approximation), while the convolutions arising due to the presence of the PML are evaluated (using TRC, which is a second-order approximation [22]) at $(n+1)\Delta t$.

From the above, Maxwell's equations using CPML are rewritten in a discretized form using a second-order accuracy in time scheme as

$$\frac{\partial \vec{D}}{\partial t}^{n+1/2} = \nabla_\kappa \times \vec{H}^{n+1/2} + \left(\nabla_\zeta \times \vec{H}\right)^{n+1} \tag{16}$$

$$\frac{\partial \vec{B}}{\partial t}^{n+1} = -\nabla_\kappa \times \vec{E}^{n+1} - \left(\nabla_\zeta \times \vec{E}\right)^{n+3/2}. \tag{17}$$

In order to synchronize $\nabla_\zeta \times \vec{H}$ and $\nabla_\zeta \times \vec{E}$ with the main FDTD algorithm in (16) and (17), a semi-implicit scheme is used in order to derive a second-order approximation (in time) [6] of $\nabla_\zeta \times \vec{H}^{n+1/2}$ [(18)] and $\nabla_\zeta \times \vec{E}^{n+1}$ [(19)]

$$\nabla_\zeta \times \vec{H}^{n+1/2} \approx \frac{\nabla_\zeta \times \vec{H}^n + \nabla_\zeta \times \vec{H}^{n+1}}{2} \tag{18}$$

$$\nabla_\zeta \times \vec{E}^{n+1} \approx \frac{\nabla_\zeta \times \vec{E}^{n+1/2} + \nabla_\zeta \times \vec{E}^{n+3/2}}{2}. \tag{19}$$

Substituting (18) and (19) into (16) and (17), respectively, results into

$$\frac{\partial \vec{D}}{\partial t}^{n+1/2} = \nabla_\kappa \times \vec{H}^{n+1/2} + \frac{\left(\nabla_\zeta \times \vec{H}\right)^{n+1} + \left(\nabla_\zeta \times \vec{H}\right)^{n}}{2} \tag{20}$$

$$\frac{\partial \vec{B}}{\partial t}^{n+1} = -\nabla_\kappa \times \vec{E}^{n+1} - \frac{\left(\nabla_\zeta \times \vec{E}\right)^{n+3/2} + \left(\nabla_\zeta \times \vec{E}\right)^{n+1/2}}{2}. \tag{21}$$

The modified CPML stores in temporary variables the values of $\nabla_\zeta \times \vec{H}^n$ and $\nabla_\zeta \times \vec{E}^{n+1/2}$ and subsequently calculates $\nabla_\zeta \times \vec{H}^{n+1}$ and $\nabla_\zeta \times \vec{E}^{n+3/2}$ according to [12]. The second-order semi-implicit approximations in (18) and (19) can now be trivially calculated and added as correction terms in the CPML-FDTD code. From the above, it is evident that no additional variables are needed to be stored compared to CPML.

It is evident from (20) that the synchronized CPML remains a media agnostic formulation as it is independent of the electric flux $\vec{D}$. Therefore, the presence of dispersive or lossy media cannot affect the suggested synchronization.

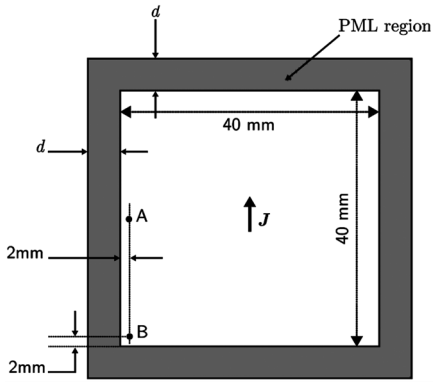

Fig. 1. y-directed current source is located at the center of a 40×40 TE_z FDTD grid. The electric field E_y is probed at A and B points. The spatial step is $\Delta x = \Delta y = 1$ mm, and the time-step is 0.99 times the Courant limit. The thickness of the PML equals $d = 10$ mm [6].

III. Numerical Results

The performance of CPML with the proposed modification is validated through 2-D and 3-D numerical examples. The numerical experiments are similar to the ones used in [6] and [8]. The proposed algorithm, i.e., semi-implicit CPML, is compared to the standard CPML in order to show how the suggested synchronization affects the overall performance of the implemented CFS-PML. Semi-implicit CPML is also compared to the recursive integration PML (RIPML), which, as shown in [8], achieves a small increase in performance with respect to CPML.

A. Current Source Radiating in an Unbounded 2-D Region

In the first example, a TE_z (H_z, E_y, E_x) FDTD is employed. The dimensions of the model are 40×40, the discretization step equals $\Delta x = \Delta y = 1$ mm (uniform along the grid), and the time-step is 0.99 times the Courant limit. A current source is placed at the center of the grid, and the time variation of the source is equal to [6]

$$I(t) = -2\frac{t - t_0}{t_w} e^{-\left(t - \frac{t_0}{t_w}\right)^2} \tag{22}$$

where $t_w = 26.53$ ps and $t_0 = 4t_w$. The electric field E_y is sampled at A and B points (see Fig. 1). The sampled E_y fields are compared to a reference solution, and the error defined in the following equation is calculated:

$$Error|_{i,j}^{n} = 20 \cdot \log_{10} \frac{\| E|_{i,j}^{n} - E_{\text{ref}}|_{i,j}^{n} \|}{\| E_{\text{ref}_{\max}}|_{i,j} \|} \tag{23}$$

where $E|_{i,j}^{n}$ is the probed electrical field at grid points (i, j) and at n time-step, $E_{\text{ref}}|_{i,j}^{n}$ is the reference solution, and $E_{\text{ref}_{\max}}|_{i,j}$ is the maximum absolute value of the reference solution.

The thickness of the PML is 10 Yee cells, and the optimum value for $\sigma_{\max}$ is calculated according to [6]

$$\sigma_{\max} = \frac{0.8(m+1)}{Z \cdot \Delta l} \tag{24}$$

where Z is the impedance of the medium, Δl is the discretization step ($l \in \{x, y, z\}$), and $m = 3$ is the order of the polynomial function that is used to scale σ_u along the PML [6]. A constant value $\kappa_u = 1$ is applied along the FDTD. An inverse linear scaling is applied to α_u [6] with $\alpha_{max} = 0.2$. Fig. 2 illustrates the error at the receiving points A and B (see Fig. 1) using CPML, RIPML, and the semi-implicit CPML method. It is evident that there is an improvement in accuracy using semi-implicit CPML and RIPML compared to CPML. The differences regarding the accuracy between RIPML and semi-implicit CPML are negligible. The main advantage of this new semi-implicit CPML formulation is the simplicity in implementing it into existing CPML codes.

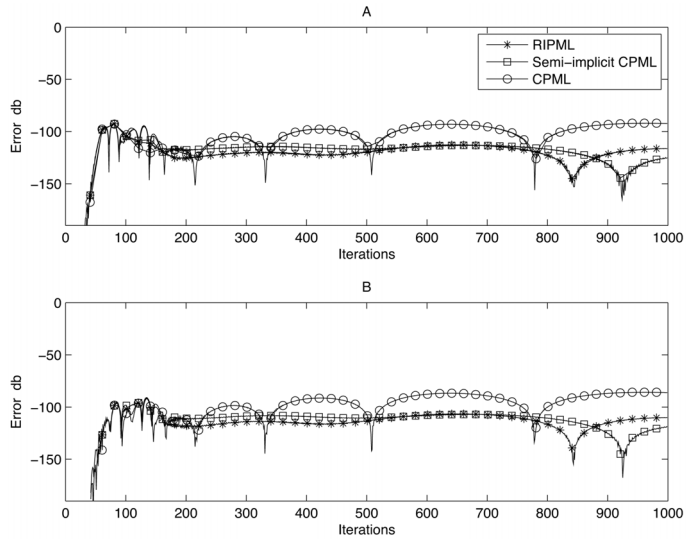

Fig. 2. Error calculated from (23) using CPML, RIPML, and semi-implicit CPML. A and B correspond to the receiving points illustrated in Fig. 1.

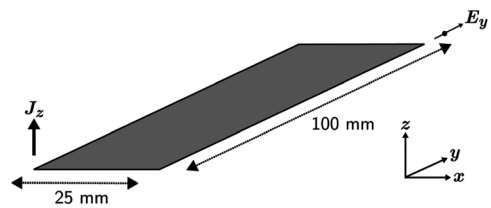

Fig. 3. z-directed Hertzian dipole over a PEC plate. The spatial step is $\Delta x = \Delta y = \Delta z = 1$ mm, and the time-step is 0.99 times the Courant limit. The thickness of the PML equals $d = 10$ mm. E_y is monitored in the opposite corner of the source's location, one Yee cell away from the PEC plate [6].

B. Current Source Over a Thin Perfect Electrical Conductor (PEC) Plate in a 3-D Domain

In the second example, the performance of the modified CPML when evanescent waves occur is examined. The dimensions of the 3-D domain are $31 \times 106 \times 6$, the discretization step is uniform along the domain and equals $\Delta x = \Delta y = \Delta z = 1$ mm, and the time-step is 0.99 times the Courant limit. A z-directed Hertzian dipole is placed on top of the edge of a 25×100-mm^2 PEC plate [8]. The time evolution of the current source is given by (22) with $t_w = 53$ ps and $t_0 = 4t_w$ [8]. The width of the PML is 10 Yee cells. The E_y-field is probed at the opposite corner from the source's location, 1 mm away from the PEC plate (see Fig. 3). The values of the stretching function are $\kappa_u = 1$ (constant along the PML), $\sigma_{\max}$ is given by (24) with $m = 3$. A linear function is used to express α_u with $\alpha_{\max} = 0.24$. Fig. 4 illustrates the error defined in (23) using CPML, semi-implicit CPML, and RIPML. It is evident that

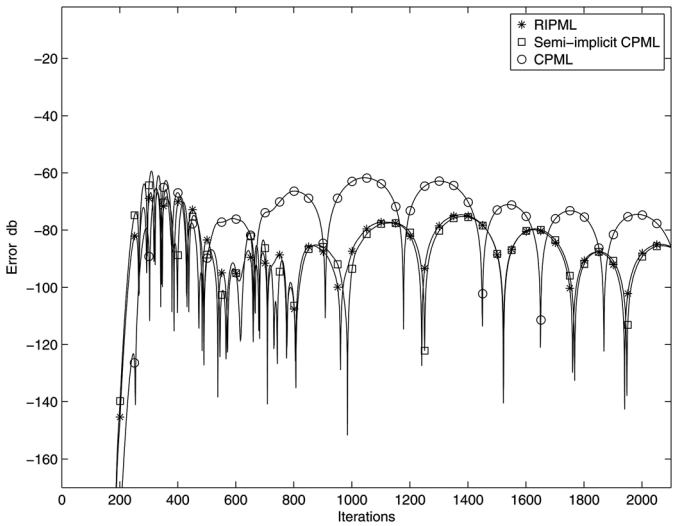

Fig. 4. Calculated error (23) using semi-implicit CPML, CPML, and RIPML for the case study described in Fig. 3.

synchronization increases the overall performance of CPML. Again, semi-implicit CPML and RIPML exhibit negligible differences in performance.

IV. Conclusion

Small differences in time synchronization between the main FDTD algorithm and the CPML implementation have an impact on the overall performance of PML absorbing boundary condition. A simple approach is suggested that resolves these performance issues by using a second-order semi-implicit approximation. The proposed modification can be implemented in a straightforward manner as a correction in a CPML-FDTD code. Numerical examples in 2-D and 3-D domains demonstrate the improvement in performance that can be achieved using the modified CPML over the original implementation.

References

[1] J. P. Berenger, "A perfectly matched layer for the absorption of electromagnetic waves," *J. Comput. Phys.*, vol. 114, pp. 185–200, 1994.

[2] W. C. Chew and W. H. Weedon, "A 3-D perfectly matched medium from modified Maxwell's equations with stretched coordinates," *Microw. Opt. Technol. Lett.*, vol. 7, no. 13, pp. 599–604, Sep. 1994.

[3] K. S. Yee, "Numerical solution of initial boundary value problems involving Maxwell's equations in isotropic media," *IEEE Trans. Antennas Propag.*, vol. AP-14, no. 3, pp. 302–307, May 1966.

[4] S. Wang, R. Lee, and F. L. Teixeira, "Anisotropic-medium PML for vector FETD with modified basis functions," *IEEE Trans. Antennas Propag.*, vol. 54, no. 1, pp. 20–27, Jan. 2006.

[5] S. D. Gedney, "An anisotropic perfectly matched layer-absorbing medium for the truncation of FDTD lattices," *IEEE Trans. Antennas Propag.*, vol. 44, no. 12, pp. 1630–1639, Dec. 1996.

[6] A. Taflove and S. C. Hagness, *Computational Electrodynamics: The Finite-Difference Time-Domain Method*, 3rd ed. Boston, MA, USA: Artech House, 2005.

[7] F. L. Teixeira and W. C. Chew, "PML-FDTD in cylindrical and spherical grid," *IEEE Microw. Guided Wave Lett.*, vol. 7, no. 9, pp. 285–287, Sep. 1997.

[8] A. Giannopoulos, "An improved new implementation of complex frequency shifted PML for the FDTD method," *IEEE Trans. Antennas Propag.*, vol. 56, no. 9, pp. 2995–3000, Sep. 2008.

[9] F. H. Drossaert and A. Giannopoulos, "A non-split complex frequency-shifted PML based on recursive integration for FDTD modeling of elastic waves," *Geophysics*, vol. 72, no. 2, pp. T9–T17, Apr. 2007.

[10] F. L. Teixeira, W. C. Chew, M. Straka, M. L. Oristaglio, and T. Wang, "Finite-difference time-domain simulation of ground penetrating radar on dispersive, inhomogeneous, and conductive soils," *IEEE Trans. Geosci. Remote Sens.*, vol. 36, no. 6, pp. 1928–1937, Nov. 1998.

[11] F. L. Teixeira and W. C. Chew, "A general approach to extend Berenger's absorbing boundary condition to anisotropic and dispersive media," *IEEE Trans. Antennas Propag.*, vol. 46, no. 9, pp. 1386–1387, Sep. 1998.

[12] J. Roden and S. Gedney, "Convolution PML (CPML): An efficient FDTD implementation of the CFS-PML for arbitrarily media," *Microw. Opt. Technol. Lett.*, vol. 27, pp. 334–339, Dec. 2000.

[13] M. Kuzuoglu and R. Mittra, "Frequency dependence of the constitutive parameters of causal perfectly matched anisotropic absorbers," *IEEE Microw. Guided Wave Lett.*, vol. 6, no. 12, pp. 447–449, Dec. 1996.

[14] E. Becache, P. G. Petropoulos, and S. D. Gedney, "On the long-time behavior of unsplit perfectly matched layers," *IEEE Trans. Antennas Propag.*, vol. 52, no. 5, pp. 1335–1342, May 2004.

[15] S. Abarbanel, D. Gottlieb, and J. S. Hesthaven, "Long time behavior of the perfectly matched layer equations in computational electromagnetics," *J. Sci. Comput.*, vol. 17, no. 1–4, pp. 405–422, Dec. 2002.

[16] J. P. Berenger, "Evanescent waves in PML's: Origin of the numerical reflection in wave-structure interaction problems," *IEEE Trans. Antennas Propag.*, vol. 47, no. 10, pp. 1497–1503, Oct. 1999.

[17] J. P. Berenger, "Numerical reflection of evanescent waves by PMLs: Origin and interpretation in the FDTD case, expected consequences to other finite methods," *Int. J. Numer. Model. Elect. Netw. Devices Fields*, vol. 13, pp. 103–114, Mar. 2000.

[18] J. P. Berenger, *Perfectly Matched Layer (PML) for Computational Electromagnetics*, 1st ed. San Rafael, CA, USA: Morgan & Claypool, 2007.

[19] R. J. Luebbers, F. Hunsberger, K. S. Kunz, R. B. Standler, and M. Schneider, "A frequency-dependent finite-difference time-domain formulation for dispersive media using FDTD," *IEEE Trans. Antennas Propag.*, vol. 44, no. 6, pp. 792–797, Jun. 1996.

[20] S. Gedney and B. Zhao, "An auxiliary differential equation formulation for the complex-frequency shifted PML," *IEEE Trans. Antennas Propag.*, vol. 58, no. 3, pp. 838–847, Mar. 2010.

[21] D. F. Kelley and R. J. Luebbers, "Piecewise linear recursive convolution for dispersive media using FDTD," *IEEE Trans. Antennas Propag.*, vol. 44, no. 6, pp. 792–797, Jun. 1996.

[22] R. Siushansian and J. LoVetri, "Efficient evaluation of convolution integrals arising in FDTD formulations of electromagnetic dispersive media," *J. Electromagn. Waves Appl.*, vol. 11, no. 1, pp. 101–117, 1997.

[23] X. Zhuansun and X. Ma, "Bilinear transform implementation of the SC-PML for general media and general FDTD schemes," *IEEE Trans. Electromagn. Compat.*, vol. 54, no. 2, pp. 343–350, Apr. 2012.

[24] J. Li and J. Dai, "Z-transform implementation of the CFS-PML for arbitrary media," *IEEE Microw. Compon. Lett.*, vol. 16, no. 8, pp. 437–439, Aug. 2006.